Biochemical and Biophysical Research Communications 383 (2009) 146–150

Contents lists available at ScienceDirect

Biochemical and Biophysical Research Communications

journal homepage: www.elsevier.com/locate/ybbrc

Purification of cytoplasmic actin by affinity chromatography using the C-terminal half of gelsolin

Takashi Ohki [a], Chikanori Ohno [a], Kotaro Oyama [a], Sergey V. Mikhailenko [b], Shin'ichi Ishiwata [a,*]

[a] Department of Physics, Faculty of Science and Engineering, Waseda University, 3-4-1 Okubo, Shinjuku-ku, Tokyo 169-8555, Japan
[b] Department of Physics, Faculty of Science, Gakushuin University, 1-5-1 Mejiro, Toshima-ku, Tokyo 171-8588, Japan

ARTICLE INFO

Article history:
Received 11 March 2009
Available online 1 April 2009

Keywords:
Actin purification
Recombinant actin
Gelsolin
Actin-binding protein
Baculovirus

ABSTRACT

A new rapid method of the cytoplasmic actin purification, not requiring the use of denaturants or high concentrations of salt, was developed, based on the affinity chromatography using the C-terminal half of gelsolin (G4–6), an actin filament severing and capping protein. When G4–6 expressed in *Escherichia coli* was added to the lysate of HeLa cells or insect cells infected with a baculovirus encoding the beta-actin gene, in the presence of Ca^{2+} and incubated overnight at 4 °C, actin and G4–6 were both detected in the supernatant. Following the addition of Ni–Sepharose beads to the mixture, only actin was eluted from the Ni–NTA column by a Ca^{2+}-chelating solution. The functionality of the cytoplasmic actins thus purified was confirmed by measuring the rate of actin polymerization, the gliding velocity of actin filaments in an *in vitro* motility assay on myosin V-HMM, and the ability to activate the ATPase activity of myosin V-S1.

Introduction

Actin filaments in living cells undergo continuous, dynamic turnover and remodeling. These processes involve polymerization, depolymerization, severing, capping, and branching of actin filaments through interaction with a vast array of actin-binding proteins. Gelsolin, a member of an actin scavenger system, rapidly severs actin filaments at substoichiometric concentrations, remaining as a cap on their barbed ends [1]. Gelsolin is composed of six repeating domains of sequence (G1–6) and contains three distinct actin binding sites, two that bind to G-actin (G1 and G4–6) and one that binds to filaments (G2) [2]. The C-terminal half (G4–6) provides the Ca^{2+}-sensitivity of gelsolin, namely, the presence of Ca^{2+} induces a significant structural rearrangement in the C-terminal half, which facilitates severing and capping of actin [3]. In the sedimentation assay [4], when F-actin was mixed for 8 h at 4 °C with G4–6 expressed in *Escherichia coli* and pelleted, the amount of actin in the supernatant increased compared with the absence of G4–6, suggesting that G4–6 induces the depolymerization of F-actin by increasing the critical concentration of actin which was capped by G4–6 in a Ca^{2+}-dependent manner.

Cytoplasmic actin has so far been purified by various methods that include cycles of polymerization/depolymerization, anion exchange, gel filtration, and DNase I or profilin affinity chromatography [5]. DNase I and profilin are the G-actin-binding proteins with the dissociation constant, K_d, of 50 pM [6] and 0.1–5 μM [7,8], respectively. The agarose column-immobilized DNase I was used to purify cytoplasmic actin from HeLa cells [9]. Due to the very high affinity for G-actin, the elution of actin from the column requires high concentration of formamide (10 M), urea (6 M), or guanidine hydrochloride (3 M), which are known to denature proteins [10,11]. Profilin is a small protein with a molecular weight of ~19 kDa, which promotes the nucleotide exchange in the actin monomers released from filaments [7]. When profilin is added to a plant-cell extract, it facilitates the depolymerization of actin filaments and forms a profilin–G-actin complex, which is then isolated by affinity chromatography on poly-L-proline-Sepharose [12]. Purified plant-actin was eluted with a high ionic strength solution (1 M KCl) followed by a G-buffer.

To eliminate the possibility of potential denaturation and structural instability of actin induced by denaturants and high concentrations of salts, we developed a rapid and gentle method of purification using the C-terminal half of gelsolin (G4–6), which was found to dissociate from actin at less than millimolar concentrations of Ca^{2+}, for isolating functional actin from the non-muscle cells.

Recombinant actins were expressed in several organisms for the mutational analysis [13,14]. Recently, Joel et al. succeeded in preparation of recombinant actins in the baculovirus/Sf9 expression system, which produces the foreign gene proteins with high levels in the insect cells [15–17]. Sf9 cells are known to be capable of post-translational modifications of eukaryotic proteins [18]. Here we expressed mouse beta-actin using baculovirus and purified it by G4–6

* Corresponding author. Fax: +81 3 5286 3437.
E-mail address: ishiwata@waseda.jp (S. Ishiwata).

0006-291X/$ - see front matter © 2009 Elsevier Inc. All rights reserved.
doi:10.1016/j.bbrc.2009.03.144

affinity chromatography. Purified recombinant beta-actin was evaluated by the ability to polymerize and interact with myosin V.

Materials and methods

Plasmid construction. The expression vector for the G4–6 construct in pCold-I (Takara Bio, Otsu, Japan) was produced as follows. The cDNA encoding G4–6 was amplified by KOD+ DNA polymerase (Toyobo, Osaka, Japan) from the mouse spleen cDNA library with a pair of oligonucleotides: 5′-gctcgagatggccgctcagcacg-3′ and 5′-cgaattctcaggcagccagctcag-3′, containing the XhoI and the EcoRI sites, respectively. The amplified cDNA was digested with XhoI and EcoRI and ligated into the pCold-I vector in the polylinker region.

The baculovirus transfer vectors for beta-actin and myosin V-HMM (1–1091 aa) and myosin V-S1 (1–807 aa) constructs were produced as follows. The cDNA encoding beta-actin was amplified by PCR from the mouse brain cDNA library with a pair of oligonucleotides: 5′-agaattcaccatggatgacgatatcgctgcg-3′ and 5′-ataagcttctagaagcacttgcggtgc-3′, containing the Kozak sequence and the EcoRI and the HindIII sites, respectively. The amplified cDNA was digested with EcoRI and HindIII and ligated into pFastBac-1 vector (Invitrogen Japan, Tokyo) in the polylinker region. The cDNA encoding myosin V (HMM or S1) was amplified by PCR from the mouse brain cDNA library with a pair of oligonucleotides: 5′-gccatggccgcgtccgagctc-3′ and 5′-tcactagtgcgctcctccaggcgactg-3′ (HMM) or 5′-tcactagtctgcatacacaggtatctcttcctt-3′ (S1). The amplified cDNA was digested with NcoI and SpeI in both cases and ligated into pFastBac-HT in the polylinker region. A myc-tag was introduced at the C-terminal end of the construct by site-directed mutagenesis. The baculoviruses encoding beta-actin and myosin V (HMM or S1) were produced by using Bac-to-Bac system (Invitrogen).

Expression and purification of recombinant proteins. *Escherichia coli* strain Rosetta 2 (DE3; Novagen, Madison, WI) was transformed by plasmid pCold-G4–6 and grown in MMI broth medium containing 0.1 mg/mL ampicillin at 37 °C to the optical density (OD 600) of 1.9. Then, the foreign protein expression was induced by refrigerating at 15 °C without isopropylthio-D-galactoside (IPTG). After cultivation at 15 °C for 12 h, the harvested cells were lysed by sonication in a binding buffer (50 mM KCl, 10 mM Tris–HCl (pH 8.0), 5 mM $CaCl_2$, 7 mM β-mercaptoethanol, 1 mM phenylmethylsulphonyl fluoride (PMSF), 0.01 mg/mL leupeptin, 1 mM ATP). Following centrifugation at 62,000*g* for 15 min, the supernatant was mixed with Ni–Sepharose 6 Fast Flow (GE Healthcare, Tokyo, Japan) beads in a conical tube on an end-to-end rotator for 60 min at 4 °C. The resin suspension was then loaded on a disposable column and washed with a 10-fold volume of a binding buffer. G4–6 was eluted with a binding buffer containing 0.2 M imidazole (pH 8.0) and dialyzed against a binding buffer.

To express recombinant myosin V-HMM, Sf9 cells were co-infected with two viruses, expressing heavy chain and light chain (calmodulin), respectively. Cells were cultured at 27 °C for 3 days, then lysed by pipetting in a lysis buffer (20 mM Tris–HCl (pH 8.0), 1 mM $MgCl_2$, 5 mM β-mercaptoethanol, 1 mM EGTA, 1 mM PMSF, 0.01 mg/mL leupeptin). Following centrifugation at 62,000*g* for 15 min, 0.3 M KCl and 5 mM ATP were added to the supernatant, and the solution was mixed with Ni–NTA agarose (Qiagen) in a conical tube on an end-to-end rotator for 60 min at 4 °C. The resin suspension was then loaded on a column and washed with a 10-fold volume of a lysis buffer containing 0.3 M KCl and 5 mM ATP. Myosin V-HMM was eluted with a lysis buffer containing 0.2 M imidazole–HCl (pH 8.0) and 40 mM KCl. Myosin V-S1 was expressed and purified similarly.

Actin purification. Skeletal actin was prepared from rabbit skeletal muscle [19]. All experimental procedures conformed to the "Guidelines for Proper Conduct of Animal Experiments" approved by the Science Council of Japan, and were approved by the Steering Committee for Animal Experimentation at Waseda University. Cytoplasmic actin used as a control of the present study was purified from HeLa cells by DNase I chromatography as described [9].

Purification of cytoplasmic and recombinant beta-actin by G4–6 affinity chromatography. HeLa cells and Sf9 cells infected with baculovirus expressing beta-actin were lysed by pipetting in a binding buffer without KCl (10 mL/2×10^7 cells), after which 50 mM KCl, 30 mM imidazole–HCl (pH 8.0), and purified G4–6 (0.4 mg/6.7×10^7 cells in case of confluent culture in 150 mm^2 culture dishes or 4 mg/8×10^7 cells in case of 40 mL suspension culture) were added and mixed at 4 °C overnight. After centrifugation at 200,000*g* for 20 min, the supernatant was mixed with Ni–Sepharose 6 Fast Flow and stirred for 60 min at 4 °C. The resin suspension was then loaded on a disposable column and washed with a 10-fold volume of a binding buffer containing 30 mM imidazole–HCl (pH 8.0). Actin was eluted with a Ca^{2+}-chelating buffer (50 mM KCl, 10 mM Tris–HCl (pH 8.0), 0.1 mM EGTA, 7 mM β-mercaptoethanol) and, after the addition of 2 mM $MgCl_2$, were further purified by one cycle of polymerization and depolymerization.

Measurement of actin-activated ATPase activity. The actin-activated ATPase activity of myosin V-HMM (0.1 μM) was determined as described [20] at 25 °C using various concentrations of actin in the solution containing 0.08 mg/mL pyruvate kinase (Sigma–Aldrich, Tokyo, Japan), 2 mM phosphoenol pyruvate (Sigma–Aldrich), 1 mM ATP, 20 mM Tris–HCl (pH 7.2), 2 mM $MgCl_2$, 40 mM KCl, 1 mM EGTA, 1 mM dithiothreitol.

In vitro motility assay. An *in vitro* motility assay was performed as described [21]. Briefly, a glass coverslip was coated with anti-c-myc antibody (Invitrogen). The surface of the coverslip was then blocked with BSA (10 mg/mL), and myosin V-HMM (2 mg/mL) was applied. The ATP concentration in the assay buffer was 1 mM. The gliding velocity of actin filaments labeled with rhodamine phalloidin was calculated from the translocation distance and the elapsed time between the successive snapshots.

Actin polymerization assay. Actin polymerization rates were measured by change in pyrenyl fluorescence upon incorporation of pyrene into actin filaments [22]. Pyrene-labeled actin (2% of total actin concentration) in G-buffer (10 mM Tris–HCl (pH 8.0),

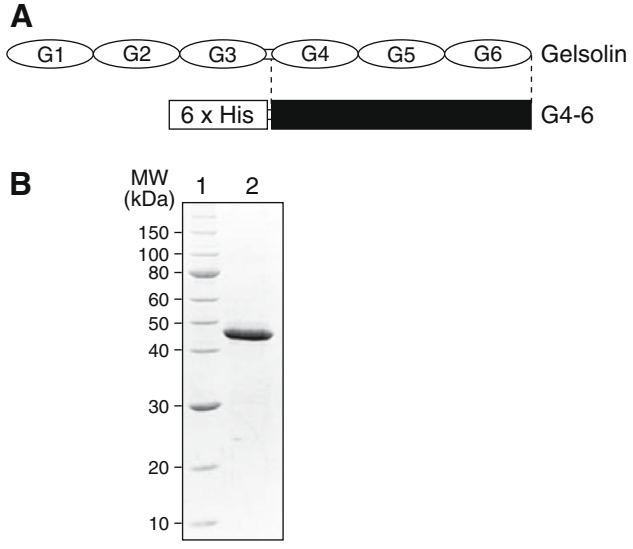

Fig. 1. Structure of gelsolin and G4–6. (A) Schematic representation of the sixfold repeating sequence of gelsolin and the deletion mutant, G4–6. (B) SDS–PAGE (12% polyacrylamide). Lane 1, molecular weight marker; lane 2, the purified G4–6. The yield was typically 150 mg/L of culture.

0.2 mM $CaCl_2$, 7 mM β-mercaptoethanol, 1 mM ATP) was pre-cleared by centrifugation at 250,000*g* for 20 min before use.

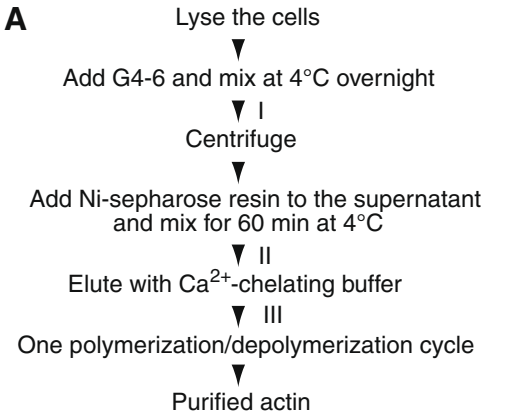

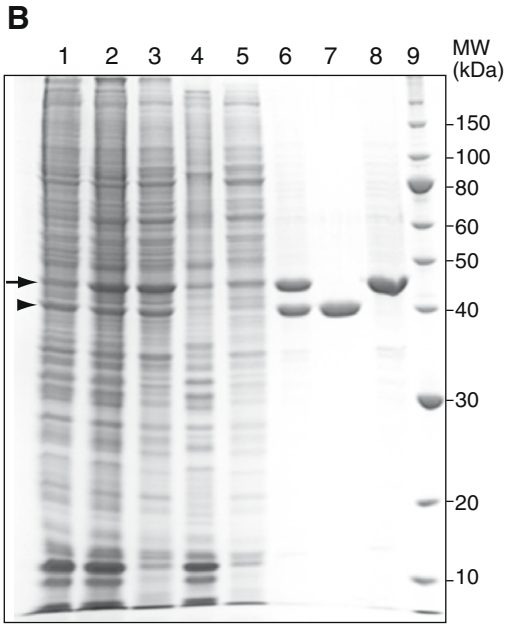

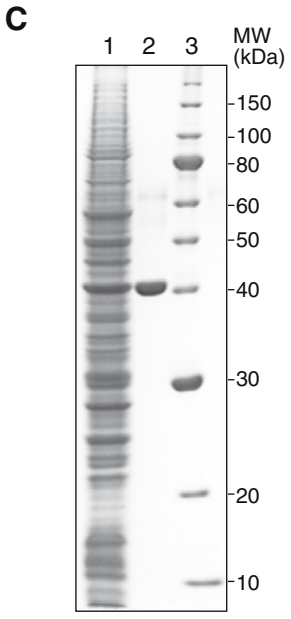

Polymerization was induced by the addition of an actin polymerization buffer (0.1 M KCl and 2 mM $MgCl_2$), and the pyrene fluorescence was monitored at 407 nm (the excitation wavelength was set at 365 nm).

Results and discussion

A new method for the rapid purification of actin

We developed a rapid and convenient method for purification of native and recombinant actins from non-muscle cells. The method uses the ability of G4–6, the C-terminal half of gelsolin, to sequester actin in a Ca^{2+}-dependent manner. This method requires only a single affinity chromatography step followed by one cycle of polymerization and depolymerization. G4–6, His_6-tagged at the N-terminal end, was expressed in *Escherichia coli* and purified by Ni–Sepharose chromatography, followed by dialysis against a binding buffer (Fig. 1B). pCold I-G4–6, the cold-shock expression vector, was expressed with high levels at 15 °C. When cells were transformed with other expression vectors carrying G4–6 gene and induced with IPTG at 37 °C, the expressed G4–6 formed aggregates. The yield was typically 150 mg/L of culture. Purified G4–6 was mixed with 50% glycerol and stored at −20 °C.

Fig. 2B shows the results from a representative cytoplasmic actin isolation procedure described by the general flow chart (Fig. 2A). Briefly, G4–6 was mixed with 6.7×10^8 HeLa cells that were lysed by pipetting in G-buffer and stirred gently at 4 °C overnight (Fig. 2A, step I, and B, lane 2). When the mixture was centrifuged at 100,000*g* for 20 min, >98% of actin was found in the supernatant (Fig. 2B, lanes 3 and 4). Ni–Sepharose beads were added to the supernatant and stirred gently for 60 min at 4 °C (Fig. 2A). The resin suspension was then loaded on a disposable column. Most of G4–6 and cytoplasmic actin was extracted from the cell lysate and retained on the Ni–Sepharose beads, as determined by SDS–PAGE (Fig. 2B, lanes 5 and 6) and immunoblotting (data not shown). After washing with a 10-fold volume of a binding buffer, actin was selectively eluted with a Ca^{2+}-chelating buffer (Fig. 2A, step II, and B, lane 7). Furthermore, G4–6 can be efficiently eluted with a Ca^{2+}-chelating buffer containing 0.2 M imidazole–HCl (pH 8.0) (Fig. 2B, lane 8) and re-used in actin purification. Actin isolated from the affinity column was further purified by a polymerization/depolymerization cycle. The yield was typically 2.2 mg/6.7×10^8 HeLa cells, while yields obtained using immobilized DNase I affinity chromatography and one cycle of polymerization and depolymerization were 1.0 mg/6.7×10^8 HeLa cells.

Mouse beta-actin was expressed without optimization of codon usage in Sf9 cells. Actin was clearly the predominant protein in the infected Sf9 cells. Following the same purification method as with HeLa cells, the recombinant actin showed no major contaminants (Fig. 2C). The yield of actin by the G4–6 affinity chromatography

Fig. 2. Actin purification by G4–6. (A) The general flow chart for actin purification using G4–6 affinity chromatography. (B) SDS–PAGE (12% polyacrylamide) of a representative actin purification experiment from HeLa cells. Lane 1, the HeLa cell lysate; lane 2, the HeLa cell lysate with the exogenous G4–6; lanes 3 and 4, the supernatant and the pellet, respectively, after centrifugation of the HeLa cell lysate with exogenous G4–6 (shown in lane 2); lane 5, a flow-through from the Ni–Sepharose column; lane 6, the fraction retained on the Ni–Sepharose column; lane 7, the fraction eluted with Ca^{2+}-chelating buffer; lane 8, the fraction eluted with Ca^{2+}-chelating buffer containing 0.2 M imidazole–HCl (pH 8.0); lane 9, the molecular weight marker. The arrow and the arrowhead show the positions of G4–6 and actin, respectively. (C) SDS–PAGE (12% polyacrylamide) of a representative mouse beta-actin purification experiment from Sf9 cells infected with baculovirus encoding beta-actin gene. Lane 1, the Sf9 cell lysate; lane 2, the beta-actin purified by G4–6 affinity chromatography; lane 3, the molecular weight marker.

was typically 32 mg/8 × 10^8 Sf9 cells (400 mL culture), which was about three times higher than when using DNase I column (12 mg/8 × 10^8 Sf9 cells).

Ca^{2+} (5 mM) is required for the formation of G4–6–actin complex in the cell lysate

Fig. 3 shows G4–6–actin complex remaining in Ni-matrix at various concentrations of Ca^{2+} determined by SDS–PAGE and immunoblotting. Earlier work reported that Ca^{2+} binds to G4–6 at a 2:1 stoichiometry and with the dissociation constants, K_d, for the two binding sites being 1.9 and 0.09 μM [4]. We therefore tested the effect of Ca^{2+} concentration on the binding between G4–6 and actin in the cell lysate. The amount of actin bound to G4–6 increased with increasing Ca^{2+} concentration and appeared to saturate at Ca^{2+} concentrations higher than 5 mM (Fig. 3C). This concentration is substantially higher than the Ca^{2+} dissociation constants for both binding sites on gelsolin, which might be caused by the competition with other actin-binding proteins present in the crude extract.

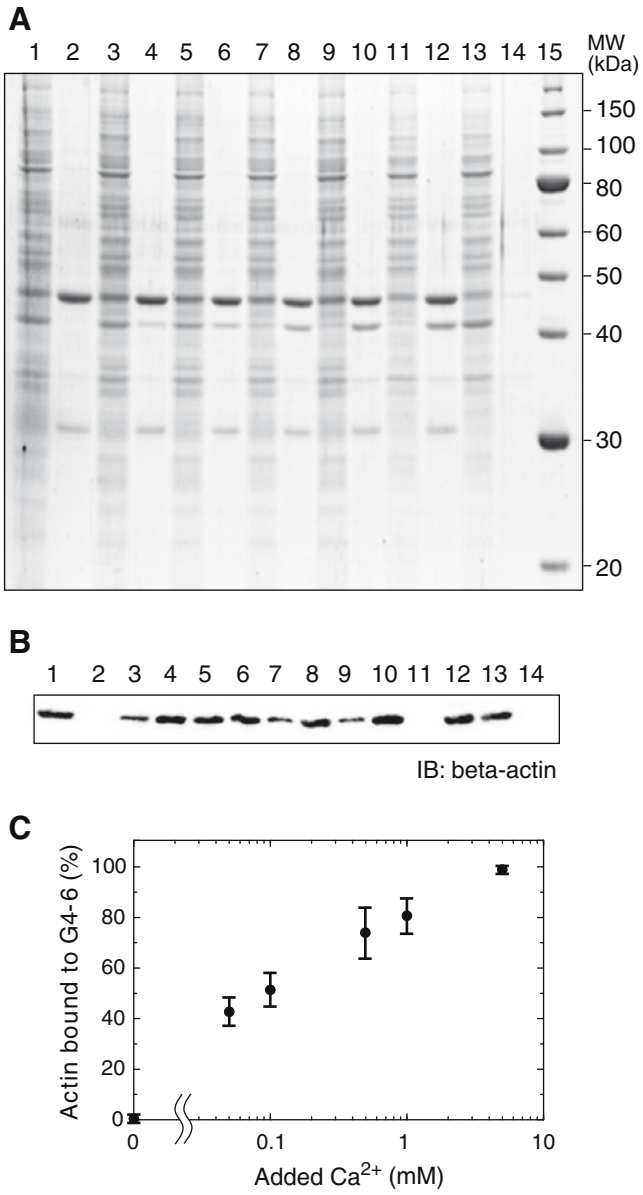

Fig. 3. Actin-binding assay. (A) Coomassie blue-stained gel of the Ni–Sepharose-bound fraction after G4–6 was mixed with the HeLa cell lysate at various concentrations of Ca^{2+} and incubated at 4 °C overnight. Lanes 1, 3, 5, 7, 9, 11, and 13 are flow-through from the Ni–Sepharose column. Lanes 2, 4, 6, 8, 10, 12, and 14 are the fractions retained on the Ni–Sepharose column. $CaCl_2$ was added at the concentrations of 0, 0.05, 0.1, 0.5, 1, and 5 mM (lanes 1–2, 3–4, 5–6, 7–8, 9–10, and 11–14, respectively). Lanes 13–14 show the same conditions as in lanes 11–12, except for the absence of G4–6. Lane 15, the molecular weight marker. (B) Immunoblot of the fractions in (A) with an anti-actin antibody (AC-15, Sigma–Aldrich). (C) The proportion of actin remained bound to Ni–Sepharose determined from the band intensities in (B). Error bars show standard deviation ($N = 3$).

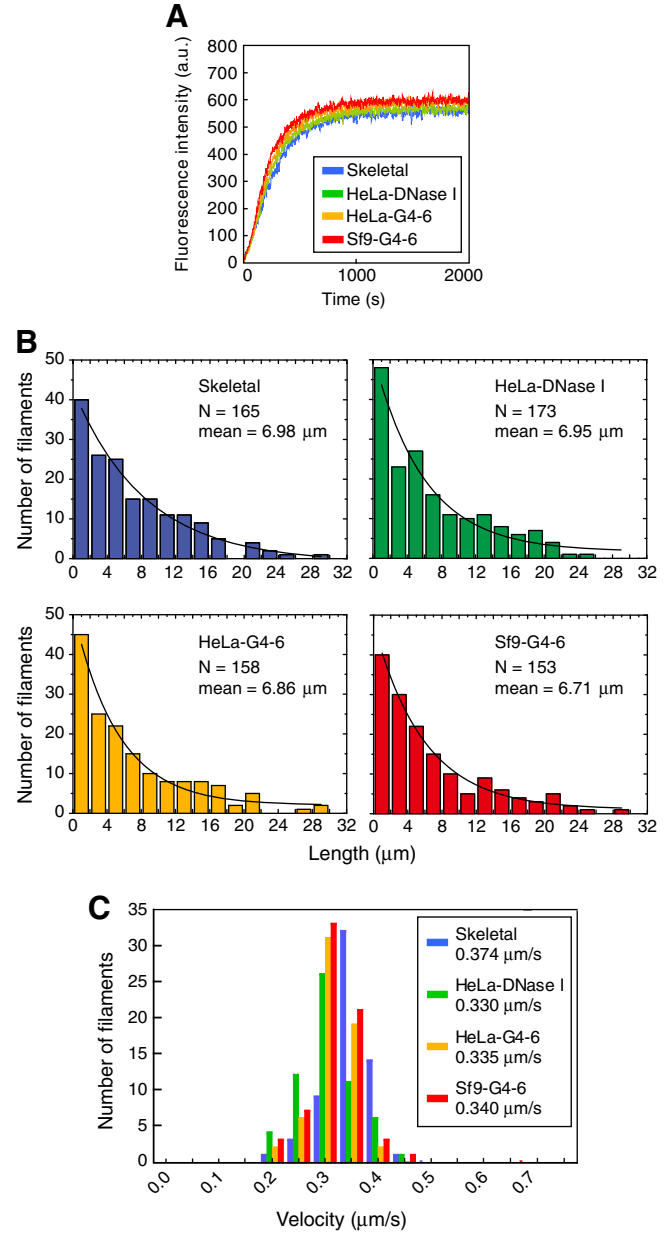

Fig. 4. Functional properties of actins purified with G4–6. (A) Polymerization of cytoplasmic and rabbit skeletal actins. Cytoplasmic actin (5 μM), containing 2% pyrene-labeled actin, in G-buffer was polymerized at 25 °C by the addition of 2 mM $MgCl_2$ and 100 mM KCl. Polymerization of rabbit skeletal actin (blue), cytoplasmic actin purified from HeLa cells by DNase I (green) and G4–6 (yellow), and recombinant beta-actin purified by G4–6 (red) was monitored as an increase in pyrenyl fluorescence intensity at 407 nm (the excitation wavelength was set at 365 nm). (B) Length distributions of rhodamine phalloidin-labeled actin filaments fitted with single exponentials. The colors correspond to those in A. (C) Distribution of the gliding velocities of rhodamine phalloidin-labeled actin filaments. Conditions: 75 mM KCl, 3 mM $MgCl_2$, 20 mM imidazole–HCl (pH 8.0), 1 mM EGTA, 1 mM ATP at 30 °C. In the inset the average velocities are shown. The colors correspond to those in (A).

Table 1
Activation of the ATPase activity of myosin V-S1 by cytoplasmic actins. Conditions: 25 °C, 0.08 mg/mL pyruvate kinase, 2 mM phosphoenol pyruvate, 1 mM ATP, 20 mM Tris–HCl (pH 7.2), 2 mM $MgCl_2$, 40 mM KCl, 1 mM EGTA, 1 mM dithiothreitol.

Actin	V_{max} (s^{-1})	K_{actin} (μM)
Skeletal	12.2 ± 0.3	6.6 ± 0.2
HeLa-DNase I	11.9 ± 0.5	6.9 ± 0.3
HeLa-G4–6	12.0 ± 0.3	6.0 ± 0.5
Sf9-G4–6	12.3 ± 0.3	6.5 ± 0.7

The values presented are the means of at least three independent experiments ± SD. Basal ATPase rate of the recombinant myosin V-S1 was $0.048 s^{-1}$ (the mean of two independent preparations).

Actins obtained by G4–6 are functional

To test whether actins purified using G4–6 affinity chromatography were functional, they were evaluated by measuring the rate of polymerization (Fig. 4A) and the filament length (Fig. 4B), and by characterizing the interaction with myosin V (Fig. 4C and Table 1). Actin polymerization was monitored as an increase in pyrenyl fluorescence intensity. When 5 μM of G-actin, containing 2% pyrene-labeled actin, was polymerized at 25 °C by the addition of 2 mM $MgCl_2$ and 100 mM KCl, the polymerization rates of actins purified by G4–6 were similar to that of rabbit skeletal actin and cytoplasmic actin purified in DNase I column (Fig. 4A). The filament lengths were measured under fluorescence microscope after labeling with rhodamine phalloidin (Fig. 4B). All detectable filaments in the samples were attached to the myosin V-HMM-coated glass in the absence of ATP. The filament length distributions were fitted with single exponentials, and the mean lengths were similar for all actins. Therefore, actin from HeLa cells and the recombinant beta-actin purified by G4–6 are both able to polymerize similarly to skeletal muscle actin, demonstrating that functional interactions between actin monomers remain intact.

The interaction with myosin V was assessed by measuring the gliding velocity of actin filaments in an *in vitro* motility assay (Fig. 4C) and the actin-activation of myosin's V ATPase activity (Table 1). All filaments in the field of view, both of the cytoplasmic and the skeletal actins, were propelled by myosin V-HMM. No significant difference in the average velocity and the velocity distribution was observed between the three cytoplasmic actins, and all three were only ~10% slower than rabbit skeletal actin (Fig. 4C). Table 1 summarizes the actin activation of the ATPase activity of myosin V-S1. The cytoplasmic actins and the skeletal actin had comparable V_{max} and K_{actin} values indicating that actins purified by G4–6 functionally interact with myosin V, which is localized in the cytoplasm of the non-muscle cells.

Thus, our new method employing G4–6, the C-terminal half of gelsolin, for the indirect isolation of actin through the trapping of the G4–6-actin complex on a Ni–Sepharose column may prove useful as a tool for rapid preparation of functional actin. The method reported here can provide a convenient source of actin for biochemical, biophysical, and structural studies of actin and the interaction with its binding partners by high-throughput mutation screening.

Acknowledgments

This work was supported by Grants-in-Aid for Scientific Research (A), the 21st Century COE Program, and "Academic Frontier" Project from the Ministry of Education, Culture, Sports, Science and Technology, Japan. This work was also supported by On-chip Cellomics Consortium, Tokyo, Japan.

References

[1] J.G. Haddad, K.D. Harper, M. Guoth, G.G. Pietra, J.W. Sanger, Angiopathic consequences of saturating the plasma scavenger system for actin, Proc. Natl. Acad. Sci. USA 87 (1990) 1381–1385.
[2] C. Chaponnier, P.A. Janmey, H.L. Yin, The actin filament-severing domain of plasma gelsolin, J. Cell Biol. 103 (1986) 1473–1481.
[3] C.G. dos Remedios, D. Chhabra, M. Kekic, I.V. Dedova, M. Tsubakihara, D.A. Berry, N.J. Nosworthy, Actin binding proteins: regulation of cytoskeletal microfilaments, Physiol. Rev. 83 (2003) 433–473.
[4] B. Pope, S. Maciver, A. Weeds, Localization of the calcium-sensitive actin monomer binding site in gelsolin to segment 4 and identification of calcium binding sites, Biochemistry 34 (1995) 1583–1588.
[5] P. Sheterline, J. Clayton, J. Sparrow, Actin, Protein Profile 2 (1995) 1–103.
[6] H.G. Mannherz, R.S. Goody, M. Konrad, E. Nowak, The interaction of bovine pancreatic deoxyribonuclease I and skeletal muscle actin, Eur. J. Biochem. 104 (1980) 367–379.
[7] C. Ampe, F. Markey, U. Lindberg, J. Vandekerckhove, The primary structure of human platelet profilin: reinvestigation of the calf spleen profilin sequence, FEBS Lett. 228 (1988) 17–21.
[8] L.A. Selden, J.E. Estes, L.C. Gershman, High affinity divalent cation binding to actin. Effect of low affinity salt binding, J. Biol. Chem. 264 (1989) 9271–9277.
[9] K. Zechel, Isolation of polymerization-competent cytoplasmic actin by affinity chromatography on immobilized DNAse I using formamide as eluant, Eur. J. Biochem. 110 (1980) 343–348.
[10] J.M. Andersland, A.T. Jagendorf, M.V. Parthasarathy, The isolation of actin from pea roots by DNase I affinity chromatography, Plant Physiol. 100 (1992) 1716–1723.
[11] K. Zechel, Dissociation of the DNAse-I actin complex by formamide, Eur. J. Biochem. 110 (1980) 337–341.
[12] B.C. Gibbon, H. Ren, C.J. Staiger, Characterization of maize (*Zea mays*) pollen profilin function in vitro and in live cells, Biochem. J. 327 (Pt 3) (1997) 909–915.
[13] P. Aspenstrom, R. Karlsson, Interference with myosin subfragment-1 binding by site-directed mutagenesis of actin, Eur. J. Biochem. 200 (1991) 35–41.
[14] M. Johara, Y.Y. Toyoshima, A. Ishijima, H. Kojima, T. Yanagida, K. Sutoh, Charge-reversion mutagenesis of Dictyostelium actin to map the surface recognized by myosin during ATP-driven sliding motion, Proc. Natl. Acad. Sci. USA 90 (1993) 2127–2131.
[15] P.B. Joel, P.M. Fagnant, K.M. Trybus, Expression of a nonpolymerizable actin mutant in Sf9 cells, Biochemistry 43 (2004) 11554–11559.
[16] C.S. Bookwalter, K.M. Trybus, Functional consequences of a mutation in an expressed human alpha-cardiac actin at a site implicated in familial hypertrophic cardiomyopathy, J. Biol. Chem. 281 (2006) 16777–16784.
[17] B.M. Miller, K.M. Trybus, Functional effects of nemaline myopathy mutations on human skeletal alpha-actin, J. Biol. Chem. 283 (2008) 19379–19388.
[18] D.R. O'Reilly, L.K. Miller, Baculovirus Expression Vectors. A Laboratory Manual, W. H. Freeman, New York, 1992.
[19] S. Uemura, H. Higuchi, A.O. Olivares, E.M. De La Cruz, S. Ishiwata, Mechanochemical coupling of two substeps in a single myosin V motor, Nat. Struct. Mol. Biol. 11 (2004) 877–883.
[20] M.E. Pullman, H.S. Penefsky, A. Datta, E. Racker, Partial resolution of the enzymes catalyzing oxidative phosphorylation. I. Purification and properties of soluble dinitrophenol-stimulated adenosine triphosphatase, J. Biol. Chem. 235 (1960) 3322–3329.
[21] T. Ohki, S.V. Mikhailenko, M.F. Morales, H. Onishi, N. Mochizuki, Transmission of force and displacement within the myosin molecule, Biochemistry 43 (2004) 13707–13714.
[22] T. Kouyama, K. Mihashi, Fluorimetry study of *N*-(1-pyrenyl)iodoacetamide-labelled F-actin. Local structural change of actin protomer both on polymerization and on binding of heavy meromyosin, Eur. J. Biochem. 114 (1981) 33–38.